Geomechanics and Engineering, *Vol. 16, No. 6 (2018) 635-642*
DOI: https://doi.org/10.12989/gae.2018.16.6.635

A simple model for ground surface settlement induced by braced excavation subjected to a significant groundwater drawdown

Runhong Zhang[3], Wengang Zhang[*1,2,3], A.T.C. Goh[4], Zhongjie Hou[3] and Wei Wang[3]

[1]*Key Laboratory of New Technology for Construction of Cities in Mountain Area, Chongqing University, Chongqing, China*
[2]*National Joint Engineering Research Center of Geohazards Prevention in the Reservoir Areas, Chongqing University, Chongqing, China*
[3]*School of Civil Engineering, Chongqing University, Chongqing, China*
[4]*School of Civil and Environmental Engineering, Nanyang Technological University, Singapore*

(Received March 9, 2018, Revised August 10, 2017, Accepted November 8, 2018)

Abstract. Braced excavation systems are commonly required to ensure stability in construction of basements for shopping malls, underground transportation and other habitation facilities. For excavations in deposits of soft clays or residual soils, stiff retaining wall systems such as diaphragm walls are commonly adopted to restrain the ground movements and wall deflections in order to prevent damage to surrounding buildings and utilities. The ground surface settlement behind the excavation is closely associated with the magnitude of basal heave and the wall deflections and is also greatly influenced by the possible groundwater drawdown caused by potential wall leakage, flow from beneath the wall, flow from perched water and along the wall interface or poor panel connections due to the less satisfactory quality. This paper numerically investigates the influences of excavation geometries, the system stiffness, the soil properties and the groundwater drawdown on ground surface settlement and develops a simplified maximum surface settlement Logarithm Regression model for the maximum ground surface settlement estimation. The settlements estimated by this model compare favorably with a number of published and instrumented records.

Keywords: ground surface settlement; logarithm regression; braced excavation; water drawdown

1. Introduction

Buildings and underground pipelines adjacent to a deep excavation are at high risks of damage due to the unfavorable ground movements. One of the main concerns in a braced excavation in an urban area is the risk of damages to adjacent infrastructures caused by the excavation-induced ground movements. Evaluating the magnitude and distribution of ground movements adjacent to a supported excavation is an important part of the design process. Although numerical modeling is a powerful tool in many design situations, it can be costly and requires considerable efforts to implement and interpret the results. Therefore, empirical/semi-empirical methods are most commonly used to predict the ground movements induced by a braced excavation.

There are many empirical and semi-empirical methods for relating the excavation induced maximum wall deflections to the basic design parameters including the excavation depth and width, the thickness of soft soils, as well as the system stiffness or the relative stiffness ratios

(Mana and Clough 1981, Wong and Broms 1989, Clough

and O'Rourke 1990, Hashash and Whittle 1996, Addenbrooke *et al.* 2000, Kung *et al.* 2007, Zhang *et al.* 2015, Goh *et al.* 2017, Xiang *et al.* 2018, Zhang *et al.* 2018a). However, when it comes to the estimation of the excavation-induced ground surface settlements, apart from the previous charts proposed last century (Peck 1969, Clough and O'Rourke 1990, Ou *et al.* 1993, Hsieh and Ou 1998), few approaches can be referred to (Hsieh and Ou 1998, Kung *et al.* 2007, Cham and Goh 2011, Zhang *et al.* 2015, Goh *et al.* 2017, Gao *et al.* 2018, Zhang *et al.* 2018b). The reasons might lie in that: firstly, the ground surface settlement response is more complicated and is generally monitored by settlement markers at different distances from behind the wall while for the wall deflection, the wall inclinometer instrumentation is much easier; secondly, it is generally accepted that the maximum ground surface settlement is generally within 0.5-1.0 time the maximum wall deflections for braced excavations (Mana and Clough 1981, O'Rourke 1981, Goh *et al.* 2017). Nevertheless, the latter is true only when the ground surface settlement is solely caused by the wall deflection through the sole deformation compatibility mechanism. For cases with considerable groundwater drawdowns behind the excavation which may be caused by potential wall leakage, flow from beneath the wall embedded in the residual soils with more percentiles of silts or sandy silts, flow from perched water and along the wall interface or poor panel connections due to less satisfactory quality, consolidation settlements are introduced due to the increased effective stresses as a result of the water drawdown, under which circumstance the measured total ground surface settlement would be much greater (Zhang and Goh 2016, Zhang *et al.* 2018c).

Ground surface consolidation settlements induced by

∗Corresponding author, Professor
E-mail: cheungwg@126.com

ISSN: 2005-307X (Print), 2092-6219 (Online)

braced excavation subjected to a significant groundwater drawdown are seldom reported and investigated systematically due to a lack of validations from case instrumentations. This paper numerically investigates the influences of excavation geometries, the system stiffness, the soil properties as well as the groundwater drawdown on the ground surface settlement using PLAXIS software and develops a simplified maximum surface settlement LR model for the maximum value estimation. The maximum ground surface settlements estimated by this model compare favorably with a number of published and instrumented records. It can provide a preliminary estimation of the ground surface consolidation settlements for braced excavations and design guidance for ongoing projects in similar ground conditions.

2. Soil model

The common soil models used in PLAXIS for braced excavation include the Mohr–Coulomb (MC) model, the hardening-soil (HS) model and the hardening-soil with small strain (HSS) model. The MC model is commonly used in practice. Based on it, the soil is elastic before failure and only switches to plastic upon reaching failure. In contrast, real soil response is elastic-plastic (i.e., nonlinear) even before failure. That is, MC model can't capture either the inelastic response or the stress-dependency behavior. The HS model is an advanced elasto-plastic strain hardening cap model for simulating the behavior of soils, especially for braced/supported excavations. The model involves frictional hardening characteristics to model plastic shear strain in deviatoric loading, and cap hardening to model plastic volumetric strain in primary compression. Failure is still defined by the Mohr-Coulomb failure criterion. Most of the soils for braced excavation are subjected to low strain levels and at low strain levels most soils exhibit a higher stiffness than at engineering strain levels for braced excavations. In addition, this stiffness varies non-linearly with strain. The main input parameters for HS model include E_{50}^{ref}, a reference secant modulus corresponding to the reference confining pressure p^{ref}, a power m for stress-dependent stiffness formulation, effective friction angle ϕ, cohesion c, failure ratio R_{f}, $E_{\text{ur}}^{\text{ref}}$ the reference stiffness modulus for unloading and reloading corresponding to p^{ref}, and υ_{ur} the unloading and reloading Poisson's ratio. This model has been used for analyses of deep excavations by a number of researchers including Finno and Calvello 2005, Bryson and Zapata-Medina 2012, Goh *et al.*2017, Zhang *et al.* 2017, Xiang *et al.*2018, Zhang *et al.* 2018d, Zhang *et al.* 2018e.

The HSS model is an improvement based on the HS model, accounting for the increased stiffness of soils at small strains with introduction of two additional parameters which are G_0^{ref} and $\gamma_{0.7}$. G_0^{ref} is a reference initial shear stiffness corresponding to the reference pressure p^{ref} and shear strain $\gamma_{0.7}$ at which the secant shear modulus is reduced to 70% of G_0. The reader can refer to Benz (2007) for additional details. Since the chart for estimating the parameter $\gamma_{0.7}$ based on Vucetic and Dobry (1991) and reported in Brinkgreve *et al.* (2006) shows that $\gamma_{0.7}$ only varies within a narrow of range of between 1×10^{-4} and 4×10^{-4}, in this paper $\gamma_{0.7}= 2\times10^{-4}$ was assumed. The G_0 is defined as

$$G_0 = G_0^{ref}\left(\frac{ccos\phi - \sigma_1' sin\phi}{ccos\phi + p^{ref} sin\phi}\right)^m \quad (1)$$

where σ_1' is the major principal effective stress. Following the approach recommended by Brinkgreve *et al.* (2006), G_0 was obtained by firstly determining the E_0/E_{ur} ratio based on the chart by Alpan (1970) and assuming $E_{\text{ur}} = 3E_{50}$. The effective friction angle is computed using the correlation proposed by Wroth and Houlsby (1985)

$$\frac{c_u}{\sigma_v'} = 0.5743\frac{3sin\phi}{3 - sin\phi} \quad (2)$$

in which c_{u} is the undrained shear strength and σ'_{v} is the vertical effective stress. When the groundwater table is at the ground surface and assuming m = 1, $c_{\text{u}}/\sigma'_{\text{v}} = \alpha$, soil stiffness ratio $E_{50}/c_{\text{u}} = \beta$ and $\sigma_3' = K_0\sigma_1'$ in the HSS model, E_{50}^{ref} can be expressed as (Zhang *et al.* 2015)

$$E_{50}^{ref} = \frac{E_{50}}{\left(\frac{\sigma_3'}{p^{ref}}\right)^m} = \frac{\alpha c_u}{\left(\frac{K_0 \times c_u}{\beta \times p^{ref}}\right)^m} = \frac{\alpha\beta p^{ref}}{K_0} \quad (3)$$

The HSS model accounts for the increased stiffness of soils at small strains. At low strain levels most soils exhibit a higher stiffness than at engineering strain levels, and this stiffness varies non-linearly with strain. In the back analysis for the TNEC case history, Kung *et al.* (2009) used a small-strain constitutive model as well as a Modified Cam Clay (MCC) model for soft/medium clay. Their results indicated that the small-strain model was able to predict the wall lateral deflection and ground surface settlement fairly well, but that the MCC model could not predict accurately the surface settlement. Other publications in which small strain has been used to model excavation in soft/medium clay include Hashash and Whittle (1996), Jen (1998), Kung (2003), Finno and Tu (2006), Kung *et al.* (2007), Lam (2010), Clayton (2011), and Zhang *et al.* (2015).

The Plaxis default values are used to define the power for stress-level dependency of the stiffness m, the coefficient of earth pressure at-rest K_0^{nc}, the Poisson's ratio υ_{ur} and E_{ur} with m = 1, K_0^{nc} = 1 – sin, υ_{ur} = 0.2 and $E_{\text{ur}} = 3E_{50}$.

3. Finite element analysis

Parametric studies have been carried out using the HSS model for the soft clay with emphasis on the ground surface settlements. Fig. 1 shows schematically the cross section of the excavation system, with a slightly simplified soil profile comprising of a thick normally consolidated silty clay layer overlying a stiff clay layer, typical of soil conditions in many coastal areas. The MC constitutive relationship was used to model the stiff clay (γ = 20 kN/m^3, c_u = 500 kPa, E_u = 250 MPa) underlying the soft silty clay deposit. The silty clay thickness is denoted as T in Fig. 1. The penetration depth of the wall into the stiff layer was 5 m which is proved to be sufficient against basal heave failures.

The analyses considered a plane strain excavation

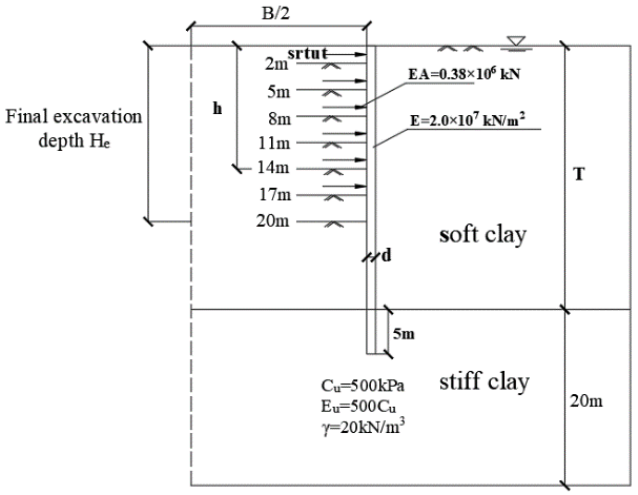

Fig. 1 Cross-sectional soil and wall profile

Table 1 Parameters considered and the values

Parameter	Ranges
Relative shear strength ratio c_u/σ'_v	0.25, 0.30, 0.35
Relative soil stiffness ratio E_{50}/c_u	100, 200, 300
Groundwater drawdown d_w (m)	0.3, 6.0, 12.0
*System stiffness S	7.309 , 8.176 , 8.846
Excavation width B (m)	30, 40
Soft clay thickness T (m)	25, 30
Excavation depth H_e (m)	14, 17, 20

*Influence of wall stiffness was studied by varying wall thickness d while keeping the Young's modulus of the wall constant (E=2.0×10^7 kN/m^2). The corresponding natural logarithm of the system stiffness ln($EI/\gamma_w h^4_{avg}$), denoted by S for the wall thickness of 0.9, 1.2 and 1.5 m with average vertical strut spacing h_{avg}=3m are 7.309 , 8.176 , 8.846, respectively.

Table 2 ϕ, K_0 and E_{50}^{ref} values for soft clay in HSS model

c_u/σ'_v		0.25	0.30	0.35
φ(°)		22.3	26.4	30.4
K_0		0.621	0.555	0.494
E_{50}^{ref} (kPa)	E_{50}/c_u =100	4026	5405	7085
	E_{50}/c_u=200	8052	10811	14170
	E_{50}/c_u =300	12077	16216	21255

supported by a retaining wall system. The soil was modeled by 15-noded triangular elements. The structural elements were assumed to be linear elastic with the wall represented by 5-noded beam elements and 3-noded bar elements were used for the 6 levels of struts located at depths of 1 m, 4 m, 7 m, 10 m, 13 m and 16 m below the original ground surface. The nodes along the side boundaries of the mesh were constrained from displacing horizontally while the nodes along the bottom boundary were constrained from moving horizontally and vertically. The right vertical boundary extends far from the excavation to minimize the effects of the boundary restraints. The ranges of properties

Table 3 Construction procedures

Phases	Construction details
Initial Phase	Generate the initial effective stress, pore pressure and state parameters.
Phase 1	Install the diaphragm wall
Phase 2	Reset displacement to zero, lowering water table inside the excavation to 2 m below ground surface, followed by the removal of soils of 2 m thickness, the water table behind the wall follows steady state seepage pattern, into the excavated area
Phase 3	Install strut at 1 m below the ground surface
Phase 4	Dewatering of 5 m and excavate to 5 m below the ground surface inside the excavation
Phase 5	Install strut at 4 m below the ground surface
Phase 6	Dewatering of 8 m and Excavate to 8 m below the ground surface
Phase 7	Install strut at 7 m below the ground surface
Phase 8	Dewatering of 11 m and Excavate to 11 m below the ground surface
Phase 9	Install strut at 10 m below the ground surface
Phase 10	Dewatering of 14 m and Excavate to 14 m below the ground surface
Phase 11	Install strut at 13 m below the ground surface
Phase 12	Dewatering of 17 m and Excavate to 17 m below the ground surface
Phase 13	Install strut at 16 m below the ground surface
Phase 14	Dewatering of 20 m and Excavate to 20 m below the ground surface

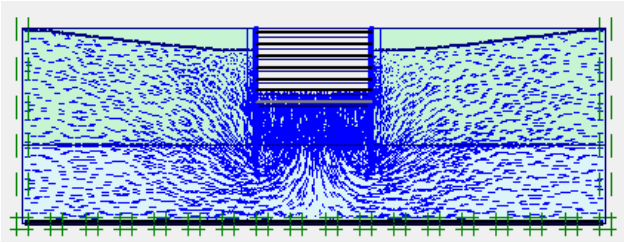

Fig. 2 Groundwater drawdown pattern (d_w=6 m)

varied are shown in Table 1. The various φ, K_0, and E_{50}^{ref} values derived from the commonly used empirical equations (Zhang *et al.* 2015, Liang and Jia 2017) are listed in Table 2.

The strut stiffness per meter EA is assumed as a constant at 3.80×10^6 kN/m since the influence of strut stiffness on wall deflection is not very significant when the strut is stiff (Poh and Wong 1997). A total of 746 hypothetical cases were analyzed.

The construction sequence comprised the following steps:

(1) the wall is installed ("wished into place") without any disturbance in the surrounding soil;

(2) the soil is excavated uniformly 1 m below each strut level prior to adding the strut support with struts at 3 m vertical spacing until the final depth H_e is reached. Details are listed in Table 3.

The groundwater table was at the ground level when excavation started. As excavation proceeds, the water head inside the excavation drops to the excavation level with each stage. Meanwhile, the groundwater drawdown outside excavation may be caused by wall leakage, flow from

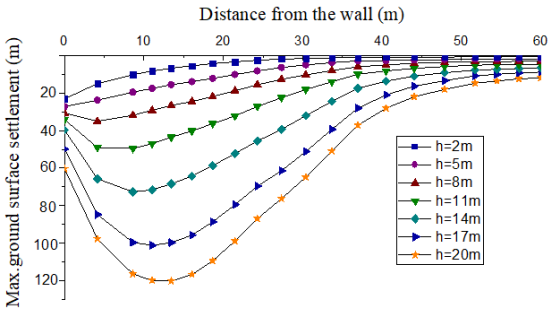

Fig. 3 Max ground surface settlements δ_{vm} for different excavation stages

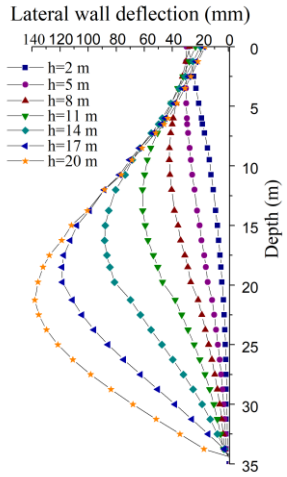

Fig. 4 Max. wall deflection δ_{hm_w} for different excavation stage

beneath wall and perched water, flow along wall interface or poor D-wall panel connections. The maximum drawdown is considered as 12 m, 6 m and 0.3 m, respectively. The drawdown curve is determined through the steady state seepage pattern, as shown in Fig. 2. It is obvious that due to the hydraulic head difference, the water behind the excavation flows into the excavated area through the zones right below the final elevation level (Wen and Lin 2002).

Fig. 3 shows the ground surface settlement profiles corresponding to the different excavation stages for case of B=30 m, H_e=20 m, c_u/σ'_v=0.35, E_{50}/c_u=200, S=8.176, d_w=6.0 m and T=30 m. It is obvious that the maximum ground surface settlement δ_{vm} increases as excavation proceeds. In addition, the ground surface settlement trough widens as excavation proceeds. For excavation depth h of 2 m, the width of the settlement trough is about 25 m. It increases to about 50 m when the excavation depth h is 11 m. It should also be noted that the maximum ground surface settlement at the final elevation level increases from 90.6 mm to 120.4 mm, compared with the case without consideration of groundwater drawdown, indicating that the consolidation settlement induced by the increased effective stress due to groundwater drawdown is considerable. Fig. 4 shows the corresponding maximum wall deflections for each excavation stage. It is obvious that the wall deflects more as excavation proceeds.

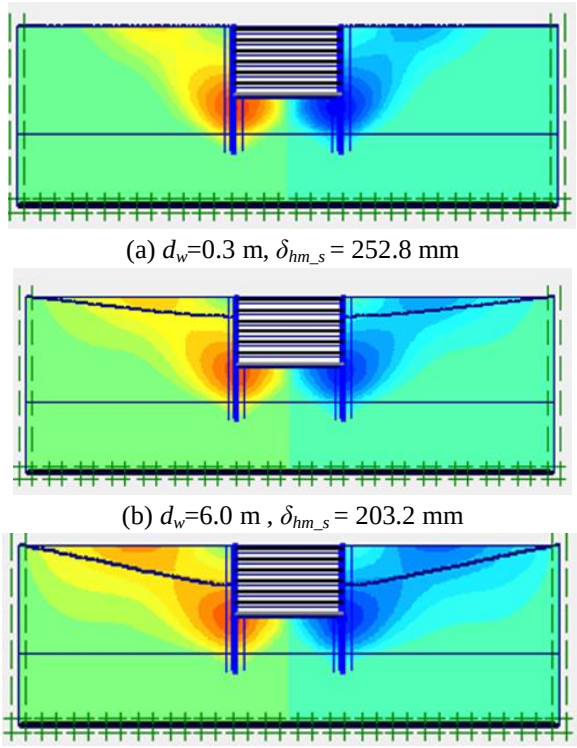

(a) d_w=0.3 m, δ_{hm_s} = 252.8 mm

(b) d_w=6.0 m , δ_{hm_s} = 203.2 mm

(c) d_w=12.0 m, δ_{hm_s} = 151.0 mm

Fig. 5 Ground horizontal movement for different groundwater drawdown d_w

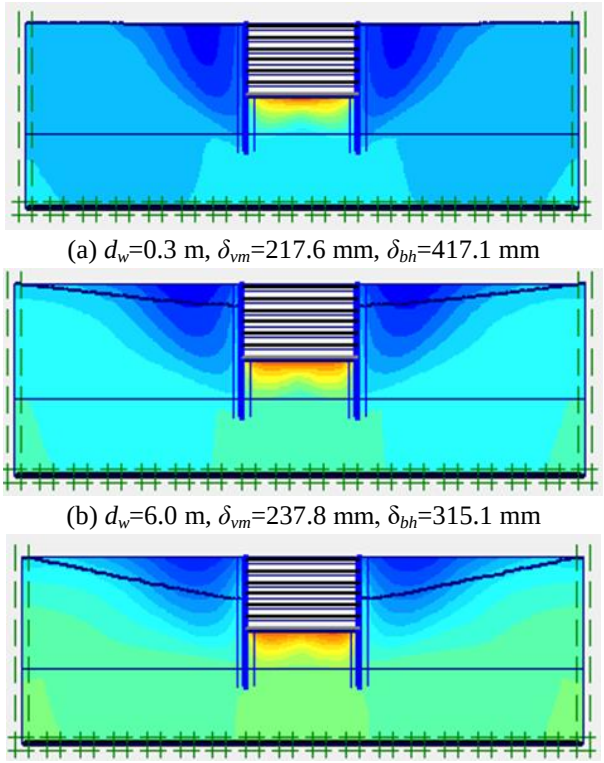

(a) d_w=0.3 m, δ_{vm}=217.6 mm, δ_{bh}=417.1 mm

(b) d_w=6.0 m, δ_{vm}=237.8 mm, δ_{bh}=315.1 mm

(c) d_w=12.0 m, δ_{vm}=261.5 mm, δ_{bh}=230.6 mm

Fig. 6 Ground surface settlements for different ground water drawdown d_w

Fig. 5 shows the influence of the groundwater drawdown on the soil lateral movement behind the wall,

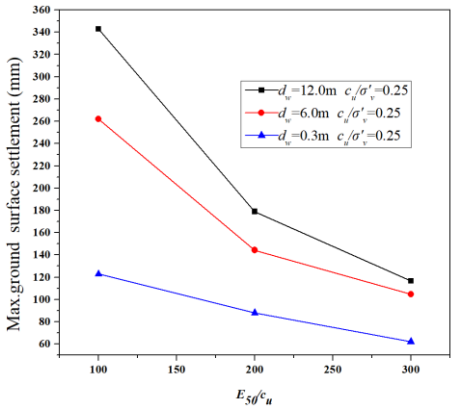

(a) Influence of E_{50}/c_u and d_w on δ_{vm} for c_u/σ'_v=0.25

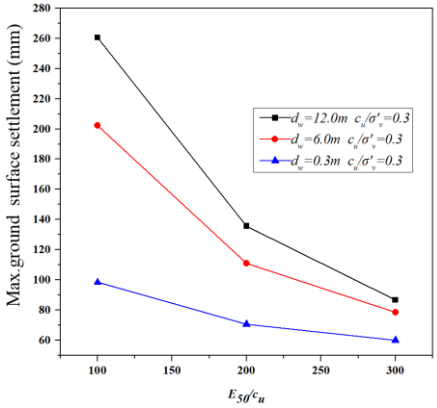

(b) Influence of E_{50}/c_u and d_w on δ_{vm} for c_u/σ'_v=0.3

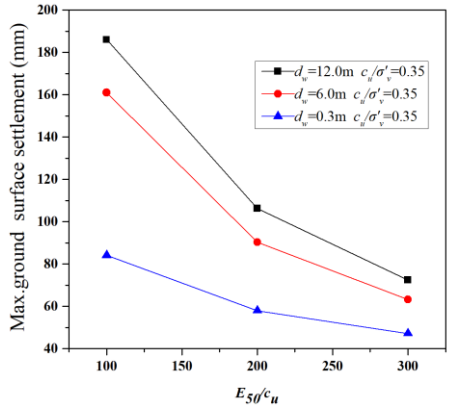

(c) Influence of E_{50}/c_u and d_w on δ_{vm} for c_u/σ'_v=0.35

Fig. 7 Effect of soil shear strength ratio and water drawdown on Max. ground surface settlement

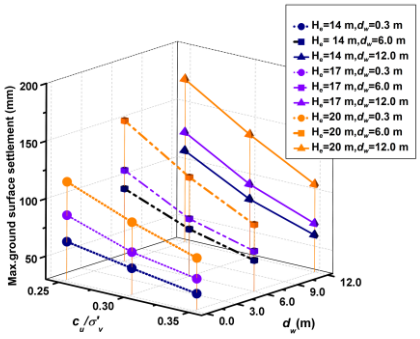

Fig. 8 Effect of excavation depth and water drawdown on Max. ground surface settlement

for cases with B=30 m, T=30 m, H_e=20 m, S=7.309, c_u/σ'_v=0.30, E_{50}/c_u=200, under d_w=0.3 m, 6.0 m and 12.0 m, respectively. It is obvious that for the same excavation depth, the more water drawdown, the less the maximum lateral soil movement (δ_{hm_s}) behind the wall due to a decreased pore water pressure acted on the wall. Accordingly, the diaphragm wall, as well as the soil behind deflects less.

Fig. 6 shows the influence of groundwater drawdown on the ground settlement profiles, the maximum ground surface settlement δ_{vm} and the basal heaves δ_{bh}, for cases with B=30 m, T=30 m, H_e =17 m, S=7.309, c_u/σ'_v=0.30, E_{50}/c_u=200, under d_w = 0.3 m, 6.0 m and 12.0 m, respectively. It is obvious that δ_{vm} increases significantly as the water drawdowns more. Fig. 6 also indicates that the settlement trough widens as the groundwater drawdown increases from 0.3 to 12.0 m, which confirms the finding in Fig. 2. In addition, the basal heaves δ_{bh} decrease considerably since the uplift pressures exerted on basal soils are reduced due to the groundwater drawdowns.

Fig. 7 shows the influence of the soil shear strength ratio c_u/σ'_v and the groundwater drawdown d_w on the maximum ground surface settlement, for cases with B=30 m, T=30 m, H_e=14m, S=8.846 for c_u/σ'_v=0.25, 0.3, 0.35, d_w = 0.3 m, 6.0 m and 12.0 m, respectively. It is obvious that the max. ground settlement increases as the soil shear strength ratio c_u/σ'_v is becoming smaller and the groundwater drawdown becomes more significant. In addition, for the same c_u/σ'_v and d_w, the max.ground settlement decreases as the relative soil stiffness ratio increases.

For brevity, only some general trends of the ground surface settlements are highlighted. The influence of the soil stiffness ratio E_{50}/c_u and the shear strength ratio c_u/σ'_v is shown in Fig. 7, for cases with B=30 m, T=25 m, H_e=17 m, S=8.176 for d_w = 0.3 m, 6.0 m and 12.0 m, respectively. It is obvious that the max. ground surface settlement decreases with the increase of the relative soil stiffness ratio E_{50}/c_u and the relative soil shear strength ratio c_u/σ'_v.

Fig. 8 shows the influence of the excavation depth H_e and the groundwater drawdown d_w on the maximum ground surface settlement, for cases with B=30 m, T=30 m, S=8.176 for H_e =14 m, 17 m, 20m, d_w = 0.3 m, 6.0 m and 12.0 m, respectively. It is obvious that the max. ground settlement increases as the excavation is becoming deeper and the groundwater drawdown becomes more significant.

4. Estimation model

Based on the numerical results and the least-square method, a simple Logarithm Regression (LR) model has been developed for estimating the maximum ground surface settlement δ_{vm}, as a function of seven input parameters of excavation geometries B, T, H_e, soil parameters c_u/σ'_v, E_{50}/c_u, system stiffness S, and groundwater drawdown d_w. The optimal equation with coefficient of determination R^2=0.9245 for δ_{vm} takes the following form

$$\delta_{vm}=24.26B^{0.3747}T^{0.7251}(H_e)^{1.2032}(c_u/\sigma'_v)^{-1.4687}(E_{50}/c_u)^{-0.5479}S^{-2.2223}(d_w)^{0.1013} \quad (4)$$

Table 4 Summary of excavation case histories

Case No.	Name	B (m)	T (m)	H_e (m)	c_u/σ'_v	E_{50}/c_u	S	d_w (m)	δ_{vm_m} (mm)	δ_{vm_LR} (mm)
1	tunnel at Race Course Road (Wen and Lin 2002)	14	12.0	17.4	0.25	200	8.110	11.3	51.0	63.0
2	Cashew station section 4	50	3.0	19.5	0.35	200	6.158	12.7	42.0	48.5
3	Cashew station section 8	30	6.9	19.5	0.35	200	6.158	13.5	87.0	73.8
4	Cashew station section 9	30	12.5	19.5	0.35	200	6.158	13.6	118.3	113.6
5	Cashew station section 13	30	8.7	19.5	0.35	200	6.158	13.1	71.7	87.0
6	Hillview station section 7	36	7.0	24.5	0.35	200	8.836	12.8	25.9	46.8
7	Hillview station section 9	40	7.5	24.5	0.35	200	8.836	13.1	28.0	51.3
8	Hillview station section 12	40	13.0	24.5	0.35	200	8.836	14.1	69.5	77.1
9	Hillview station section 13	40	3.0	24.5	0.35	200	8.836	13.0	14.9	26.4
10	Hillview station section 14	40	25	24.5	0.35	200	8.836	16.1	171.2	125.5
11	Hillview station section 16	40	7.5	24.5	0.35	200	8.836	12.8	31.7	51.2
12	Hillview station section 19	18	8.5	24.5	0.35	200	8.836	7.8	48.2	39.5
13	BKP section 1	54	6.2	20.0	0.35	200	8.176	4.7	48.2	42.0
14	BKP section 5	30	5.8	20.0	0.35	200	8.176	4.4	33.0	31.9
15	BTW section 3	70	4.9	21.0	0.35	200	8.176	3.1	52.0	39.7
16	BTW section 4	70	8.5	21.0	0.35	200	8.176	6.5	54.0	63.7
17	BTW section 5	45	5.6	21.0	0.35	200	8.176	4.2	25.0	38.2
18	BTW section 7	45	4.2	21.0	0.35	200	8.176	2.0	37.0	28.8
19	BTW section 8	45	5.1	21.0	0.35	200	8.176	6.3	41.0	37.2

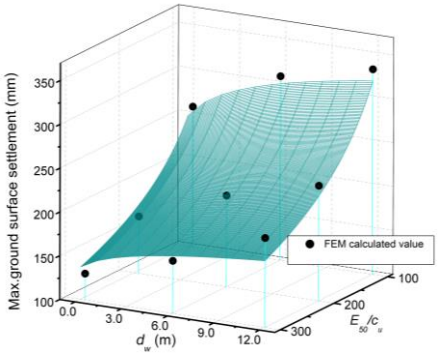

Fig. 9 Response surface for d_w and E_{50}/c_u and points of the FEM results

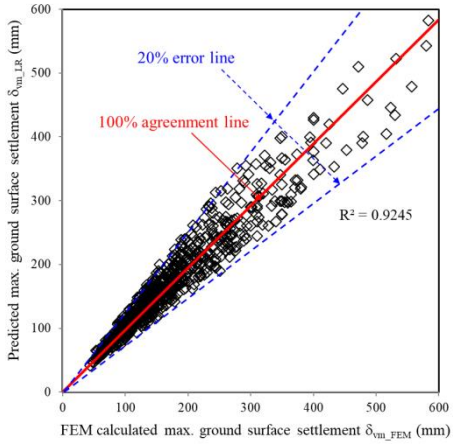

Fig. 10 Comparison between δ_{vm_LR} and δ_{vm_FEM}

Based on the expression for δ_{vm}, the system stiffness S is the most influential parameter since its absolute power value is the greatest, followed by the relative shear strength ratio c_u/σ'_v and the excavation depth H_e. Fig. 9 shows the plot of the estimation model of the maximum ground surface settlement, for cases with B=30 m, T=30 m, H_e =17m, S=8.176 assuming the d_w and E_{50}/c_u change within the assigned ranges. Also plotted in Fig. 9 are the 9 data points from FEM for d_w=0.3 m, 6.0 m and 12.0 m, E_{50}/c_u=100, 200, 300 respectively.

Fig. 10 shows the plot of the maximum ground surface settlement estimations using Eq. (4) versus the FEM values for the 746 hypothetical cases, indicating that Eq. (4) is reasonably accurate since most of the points are enveloped by the 20% error line.

5. Validation of the proposed LR model

To validate the proposed LR model, a total of 19 well-documented excavation case histories as listed in Table 4

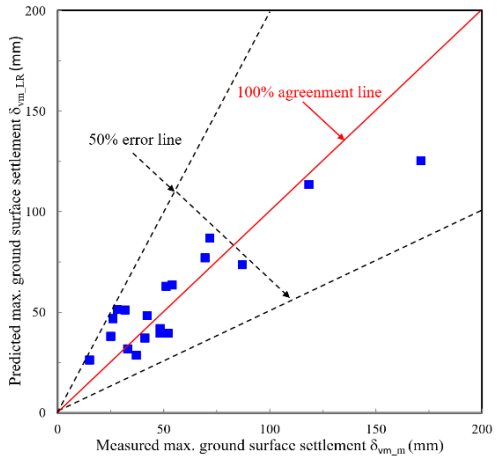

Fig. 11 Comparison between δ_{vm_LR} and δ_{vm_m}

were utilized. It should be noted that references with groundwater drawdown recordings are rarely reported. Fig. 11 shows the predicted maximum ground surface settlement δ_{vm_LR} versus the measured δ_{vm_m} values for the 19 cases represented by the blue solid squares. The plot indicates that the developed LR model is able to predict reasonably well (within relative error of 50%) the excavation induced maximum ground surface settlements for the case histories considered, though many other influential factors such as the soil profiles, construction sequences, the workmanship, etc., are not taken into consideration.

6. Conclusions

This paper presents a semi-empirical LR model for estimating the maximum ground surface settlements for braced excavations in clays in which the wall penetrates into a stiff stratum. This proposed LR model relates the maximum ground surface settlements to the various influential parameters including the excavation geometries, the system stiffness, the soil properties and the groundwater drawdown. Well-documented case histories demonstrating the reliability of the proposed LR model are given. This proposed simple LR model can be used for a preliminary estimation of the maximum ground surface settlement induced by braced excavation subjected to a significant groundwater drawdown.

It should be noted that the proposed model should be used in similar soil stratigraphy, i.e., soft clay layer underlain by stiff clays. For grounds with great thickness of soft to medium clays, or soil-rock mixture ground conditions, this model should be used with caution.

Acknowledgements

The authors are grateful to the financial support from the National Natural Science Foundation of China (51608071), the Financial grant from the China Postdoctoral Science Foundation (2017M620414), the sponsorship by Natural Science Foundation of Chongqing, China (cstc2018jcyjAX0632), the Special Funding for Postdoctoral research projects in Chongqing (No. Xm2017007) and the Advanced Interdisciplinary Special Cultivation program (No. 106112017CDJQJ208850).

References

Addenbrooke, T.I., Potts, D.M. and Dabee, B. (2000), "Displacement flexibility number for multiple retaining wall design", *J. Geotech. Geoenviron. Eng.*, **126**(8), 718-726.

Alpan, I. (1970), "The geotechnical properties of soils", *Earth-Sci. Rev.*, **6**(1), 5-49.

Benz, T. (2007), "Small-strain stiffness of soil and its numerical consequences", Ph.D. Thesis, University of Stuttgart, Stuttgart, Germany.

Brinkgreve, R.B.J., Broere, W. and Waterman, D. (2006), *PLAXIS version 8.5 Manual*, AA Balkema, Rotterdam, The Netherlands.

Bryson, L.S. and Zapata-Medina, D.G. (2012), "Method for estimating system stiffness for excavation support walls", *J. Geotech. Geoenviron. Eng.*, **138**(9), 1104-1115.

Cham, W.M. and Goh, K.H. (2011), "Prediction of ground settlement due to adjacent deep excavation works", *Proceedings of the Underground Singapore 2011*, Singapore, December.

Clayton, C.R.I. (2011), "Stiffness at small strain: Research and practice", *Géotechnique*, **61**(1), 5-37.

Clough, G.W. and O'Rourke, T.D., (1990), *Construction Induced Movements of In-Situ Walls*, in *Design and Performance of Earth Retaining Structure* in *Geotechnical Special Publication No. 25, ASCE*, New York, U.S.A., 439-470,.

Finno, R.J. and Calvello, M. (2005), "Supported excavations: The observational method and inverse modeling", *J. Geotech. Geoenviron. Eng.*, **131**(7), 826-836.

Finno, R.J. and Tu, X.X. (2006), "Selected topics in numerical simulation of supported excavations", *Proceedings of the International Conference on Numerical Simulation of Construction Processes in Geotechnical Engineering for Urban Environment*, Bochum, Germany, March.

Gao, X., Liu, H., Zhang, W., Wang, W. and Wang, Z. (2018), "Influences of reservoir water level drawdown on slope stability and reliability analysis", *Georisk*, 1-9.

Goh, A.T.C., Zhang, F., Zhang, W.G., Zhang, Y.M. and Liu, H.L. (2017), "A simple estimation model for 3D braced excavation wall deflection", *Comput. Geotech.*, **83**, 106-113.

Hashash, Y.M.A. and Whittle, A.J. (1996), "Ground movement prediction for deep excavations in soft clay", *J. Geotech. Eng.*, **122**(6), 474-486.

Hsieh, P.G. and Ou, C.Y. (1998), "Shape of ground surface settlement profiles caused by excavation", *Can. Geotech. J.*, **35**(6), 1004-1017.

Jen, L.C. (1998), "The design and performance of deep excavation in clay", Ph.D Thesis, Massachusetts Institute of Technology. Cambridge, Massachusetts, U.S.A.

Kung, G.T.C. (2003), "Surface settlement induced by excavation with consideration of small-strain behavior of Taipei silty clay", Ph.D. Thesis, National University of Science and Technology, Taipei, Taiwan.

Kung, G.T.C., Hsiao, E.C.L. and Juang, C.H. (2007), "Evaluation of a simplified small-strain soil model for analysis of excavation-induced movements", *Can. Geotech. J.*, **44**(6), 726-736.

Kung, G.T.C., Juang, C.H., Hsiao, E.C.L. and Hashash, Y.M.A. (2007), "Simplified model for wall deflection and ground-surface settlement caused by braced excavation in clays", *J. Geotech. Geoenviron. Eng.*, **133**(6), 731-747.

Kung, G.T.C., Ou, C.Y. and Juang, C.H. (2009), "Modeling small-strain behavior of Taipei clays for finite element analysis of braced excavations", *Comput. Geotech.*, **36**(1), 304-319.

Lam, S.S.Y. (2010), "Ground movements due to excavation in

clay: Physical and analytical models", Ph.D. Thesis, University of Cambridge, Cambridge, U.K.
Liang, F.Y. and Jia, Y.J. (2017), "Experimental study on parameters of HSS model for soft soils in Shanghai", *Chin. J. Geotech. Eng.*, **39**(2), 269-278.
Mana, A.I. and Clough, G.W. (1981), "Prediction of movement for braced cuts in clay", *J. Geotech. Geoenviron. Eng.*, **107**(6), 759-777.
O'Rourke, T.D. (1981) "Ground movements caused by braced excavation", *J. Geotech. Eng. Div.*, **107**(9), 1159-1178.
Ou, C.Y., Hsieh, P.G. and Chiou, D.C. (1993), "Characteristics of ground surface settlement during excavation", *Can. Geotech. J.*, **30**(5), 758-767.
Peck, R.B. (1969), "Deep excavation and tunneling in soft ground", *Proceedings of the 7th International Conference on Soil Mechanics and Foundation Engineering*, Mexico City, Mexico.
Poh, T.Y., Wong, I.H. and Chandrasekaran, B. (1997), "Performance of two propped diaphragm walls in stiff residual soils", *J. Perform. Constr. Fac.*, **11**(4), 190-199.
Vucetic, M. and Dobry, R. (1991), "Effect of soil plasticity on cyclic response", *J. Geotech. Eng.*, **117**(1), 89-107.
Wen, D.Z. and Lin, K.Q. (2002), "The effect of deep excavation on pore water pressure changes in the Old Alluvium and under-drainage of marine clay in Singapore", *Proceedings of the Geotechnical Aspects of Underground Construction in Soft Ground*, Toulouse, France, October.
Wong, K.S. and Broms, B.B. (1989), "Lateral wall deflections of braced excavation in clay", *J. Geotech. Eng.*, **115**(6), 853-870.
Wroth, C.P. and Houlsby, G.T. (1985), "Soil mechanics-property characterization and analysis procedures", *Proceedings of the 11th International Conference on Soil Mechanics and Foundations Engineering*, San Francisco, California, U.S.A., August.
Xiang, Y.Z., Goh, A.T.C., Zhang, W.G. and Zhang, R.H. (2018), "A multivariate adaptive regression splines model for estimation of maximum wall deflections induced by braced excavation", *Geomech. Eng.*, **14**(4) 315-324
Zhang, W.G. and Goh, A.T.C. (2015), "A simple prediction model for wall deflection caused by braced excavation in clay", *Comput. Geotech.*, **63**, 67-72.
Zhang, W.G. and Goh, A.T.C. (2016), "General behavior of braced excavation in Bukit Timah Granite residual soils: A case study", *Int. J. Geoeng. Case Histor.*, **3**(3), 190-202.
Zhang, W.G., Zhang, R.H. and Goh, A.T.C. (2018), "MARS inverse analysis of soil and wall properties for braced excavations in clays", *Geomech. Eng.*, In Press.
Zhang, R.H., Zhang, W.G. and Goh, A.T.C. (2018a), "Numerical investigation of pile responses caused by adjacent braced excavation in soft clays", *Int. J. Geotech. Eng.*, 1-15.
Zhang, W.G., Wang, W., Zhou, D., Goh, A.T.C. and Zhang, R. (2018b), "Influence of groundwater drawdown on excavation responses-A case history in Bukit Timah granitic residual soils", *J. Rock Mech. Geotech Eng.*, **10**(5), 856-864.
Zhang, W.G., Goh, A.T.C., Goh, K.H., Chew, O.Y.S. and Zhang, R.H. (2018c), "Performance of braced excavations in residual soils with groundwater drawdown", *Undergr. Sp.*, **3**, 150-165.
Zhang, W.G., Zhang, R.H., Fu, Y.R., Goh, A.T.C. and Zhang, F. (2018d), "2D and 3D numerical analysis on strut responses due to one-strut failure", *Geomech. Eng.*, **15**(4), 965-972.
Zhang, W.G., Hou, Z.J., Goh, A.T.C. and Zhang, R.H. (2018e), "Estimation of strut forces for braced excavation in granular soils from numerical analysis and case histories", *Comput. Geotech.*, **106**, 286-295.